

# Synthesis, Characterization and Dielectric Study of Polypyrrole/Zinc Tungstate (Ceramic) Composites

Sangappa K Ganiger<sup>1</sup>, Chaluvvaraju B V<sup>2</sup>, Murugendrappa M V<sup>3#</sup>

<sup>1</sup>Department of Physics, Government Engineering College, Raichur-584134, Karnataka, India

<sup>2</sup>Department of Physics, Bangalore Institute of Technology, Bangalore-560004, Karnataka, India

<sup>3</sup>Department of Physics, BMS College of Engineering, Bangalore-560019, Karnataka, India

**ABSTRACT:** In-situ polymerization of pyrrole (Py) was carried out with Zinc Tungstate (ceramic) in the presence of oxidizing agent ammonium persulphate to synthesize polypyrrole (PPy)/Zinc Tungstate ( $ZnWO_4$ ) by chemical oxidation method. The PPy/ $ZnWO_4$  composites were synthesized with various compositions viz., 10, 20, 30, 40 and 50 wt. % of  $ZnWO_4$  in Py. The surface morphologies of these composites were analysed using Scanning Electron Microscopy (SEM) show that  $ZnWO_4$  particles are embedded in PPy chain to form multiple phases. The Fourier Transform Infra-Red Spectroscopy (FTIR) reveals that stretching frequencies were shifted towards higher frequency side. The powder X-ray diffraction (XRD) spectrograph suggests that they exhibit semi-crystalline behaviour. Thermal analysis (TG/DTA) studies/testing were done and reported. The frequency dependent  $\epsilon'$ ,  $\epsilon''$  and tangent loss reveals that, concentration of the  $ZnWO_4$  in PPy is responsible for the variation in value of  $\epsilon'$  and  $\epsilon''$  of the composites. The dimensions of  $ZnWO_4$  particles in the matrix have a greater influence on the  $\epsilon'$  and  $\epsilon''$ .

**KEYWORDS:** Polypyrrole; Zinc Tungstate; Composites; Dielectric; Frequency.

## I. INTRODUCTION

During the last 30 years, however, conducting polymers characterized by better electrical conductivities have been found. These materials have attracted the interest of both academic and industrial researchers in fields ranging from Chemistry to Solid State Physics and Electrochemistry. The close interaction between scientists from diverse background has been major factor in the rapid development in the field of conducting polymers. The discovery of electrical conductivity in molecular charge transfer promoted the development of conducting polymers which have been synthesized and show the excellent electrical properties. Conducting polymers, by virtue of their light weight and greater ease of fabrication, have replaced and are continuing to replace metals in several areas of applications. Conducting polymers have been prepared for a wide range of applications ranging from rechargeable batteries to smart windows.

Polypyrrole (PPy) has become one of the most studied electronically conducting polymers. It can be synthesized either chemically or electro-chemically. Polypyrrole is an intrinsic conducting polymer which can be made to have conductivities up to  $1000 \text{ S cm}^{-1}$  rendering its versatile applications in batteries, electronic devices, functional electrodes, electro-chromic devices, optical switching devices, sensors and so on [1–5].

## II. LITERATURE REVIEW

Researchers have reviewed recent research work on polypyrrole type conducting polymers. Research and development work had been reviewed with special interest in chemical, electrochemical, doping process and polypyrrole based composites processes. Process development with high accuracy of product results had the direct relationship with structure and properties. According to them, polypyrrole based on a variety of structures generated from molecular structural modification could give more interesting results for future applications.

# International Journal of Innovative Research in Science, Engineering and Technology

(An ISO 3297: 2007 Certified Organization)

Vol. 3, Issue 6, June 2014

Combining two kinds of materials to form composite may lead to a synergy effect and help to enhance each other, which are helpful for improving sensor properties such as thermal stability, lower operating temperature and fast response and recovery. Conducting polymer/metal oxide nano-composites have been synthesized in most recent times and based on these nano-composites gas sensors, humidity sensors and biosensors have also been developed by few research groups. However, the conducting polymer/metal oxide based sensors are still under development and new concepts are continuously tested all over the world.

This study presents the design and fabrication of a capacitive micro humidity sensor integrated with a five-stage ring oscillator circuit on chip using the complementary metal oxide semiconductor (CMOS) process. The area of the humidity sensor chip is about  $1 \text{ mm}^2$ . The humidity sensor consists of a sensing capacitor and a sensing film. The sensing capacitor is constructed from spiral inter-digital electrodes that can enhance the sensitivity of the sensor. The sensing film of the sensor is polypyrrole, which is prepared by the chemical polymerization method, and the film has a porous structure. The sensor needs a post-CMOS process to coat the sensing film. The post-CMOS process uses a wet etching to etch the sacrificial layers, and then the polypyrrole is coated on the sensing capacitor. The sensor generates a change in capacitance when the sensing film absorbs or desorbs vapour. The ring oscillator circuit converts the capacitance variation of the sensor into the oscillation frequency output. Experimental results show that the sensitivity of the humidity sensor is about  $99 \text{ kHz}/\%R_H$  at  $25 \text{ }^\circ\text{C}$ .

## III. EXPERIMENTAL DETAILS

### SYNTHESIS

The AR grade [SpectroChem Pvt. Ltd.] pyrrole [6] was purified by distillation under reduced pressure. 0.3 M pyrrole solution was contained in a beaker which was placed in an ice tray mounted on a magnetic stirrer. 0.06 M ammonium persulphate [7] solution was continuously added drop-wise with the help of a burette to the above 0.3 M pyrrole solution. The reaction was allowed for 5 hours under continuous stirring by maintaining a temperature of  $0 \text{ }^\circ\text{C}$  to  $3 \text{ }^\circ\text{C}$ . The precipitated polypyrrole was filtered and dried in hot air oven and subsequently in a muffle furnace at  $100 \text{ }^\circ\text{C}$ . The yield of the polypyrrole was 3.6 g which has taken as 100 wt. %.

For 0.3 M pyrrole solution, 0.36 g (wt. 10%) of Zinc Tungstate ( $\text{ZnWO}_4$ ) was added and mixed thoroughly. Further 0.06 M ammonium persulphate was continuously added drop-wise with the help of a burette to the above solution to get  $\text{PPy}/\text{ZnWO}_4$  (wt. 10%) composite. Similarly, for 20, 30, 40 and 50 wt. %, 0.72 g, 1.08 g, 1.44 g and 1.8 g of  $\text{ZnWO}_4$  [Sisco Research Lab Ltd.] powder [8] is taken and the above procedure is followed to get  $\text{PPy}/\text{ZnWO}_4$  composites. The pure PPy and  $\text{PPy}/\text{ZnWO}_4$  powder was pressed in the form of pellets of 1 cm diameter using hydraulic press. The conducting silver paste was applied to the pellets of synthesized composites to act as electrodes.

### CHARACTERIZATION

The SEM [6-12] images of the pure PPy,  $\text{PPy}/\text{ZnWO}_4$  (wt. 50%) composite and  $\text{ZnWO}_4$  were recorded using Scanning Electron Microscope (Jeol 6390LV). The FTIR [6-7, 10-12] spectra of were recorded on FTIR (Thermo Nicolet Avatar 370) spectrometer in KBr medium at room temperature. The XRD patterns were recorded on X-ray Diffractometer (Bruker AXS D8 Advance) [6-11] using  $\text{Cu } k_\alpha$  radiation ( $\lambda = 1.5418 \text{ \AA}$ ) in the  $2\theta$  range  $20^\circ$ – $80^\circ$ . Thermal analysis studies/testing were done in the heat range from  $40 \text{ }^\circ\text{C}$  to  $740 \text{ }^\circ\text{C}$  at  $10 \text{ }^\circ\text{C}/\text{min}$  for the pure PPy,  $\text{PPy}/\text{ZnWO}_4$  (wt. 50%) composite and  $\text{ZnWO}_4$  using Thermal Analysis System (TG/DTA) (Perkin Elmer Diamond TG/DTA). The frequency dependent dielectric properties of our samples in the form of cylindrical pellets (1 cm dia  $\times$  1-3 mm thick, with silver paste electrodes) were studied at room temperature using Hioki (Japan) Model 3532-50 programmable computer interfaced digital LCR meter. Following parameters were selected for measurement through the LCR meter software: (1) Complex impedance,  $Z$  (ohm), (2) Phase angle  $\delta$  (degree) (3) Equivalent parallel capacitance,  $C_p$  (farad) and (4) Dissipation factor,  $D$ . About 50 frequencies,  $f$  (Hz), in the permissible range of 50 Hz to 5 MHz of the LCR meter were selected for measurement of each of these parameters. The sample was held in the sample holder and once the measurements were started, the LCR meter measured these selected parameters at each of the selected frequencies successively in 'Normal mode' which ensured higher accuracy of measurement and transferred the data to the computer. Using the measured parameters, the required parameters were calculated using the following equations, at the selected frequencies.

**RESULT AND DISCUSSION**

*SEM Analysis*

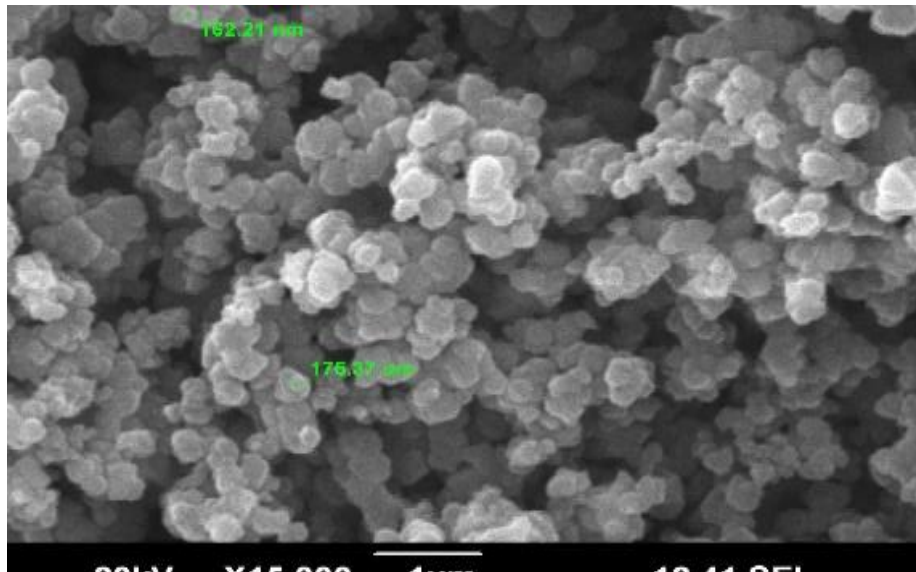


Figure 1.a SEM micrograph of the pure PPy

Figure 1.a represents the SEM micrograph of pure PPy. The figure represents the size and spherical nature of PPy particles. The elongated chain pattern of the polypyrrole particles was observed. Two particles sizes were measured as 162.21 nm and 176.37 nm.

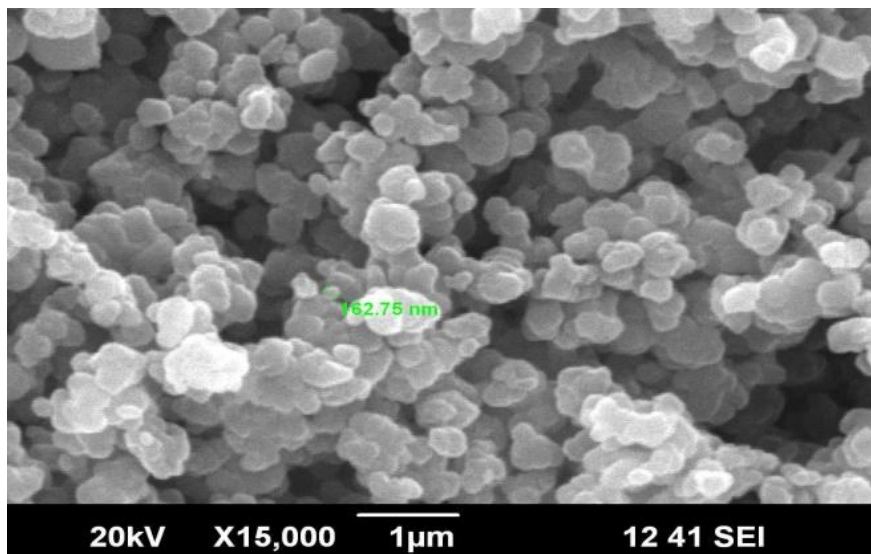


Figure 1.b SEM micrograph of the PPy/ZnWO<sub>4</sub> (wt. 50%) composite

Figure 1.b represents the SEM micrograph of the PPy/ZnWO<sub>4</sub> (wt. 50%) composite. Here, particle size was increased with small change and measured as 162.75 nm. This has shown that, the ZnWO<sub>4</sub> particles were embedded uniformly in PPy chain to form multiple phases, presumably because of weak inter-particle interactions.

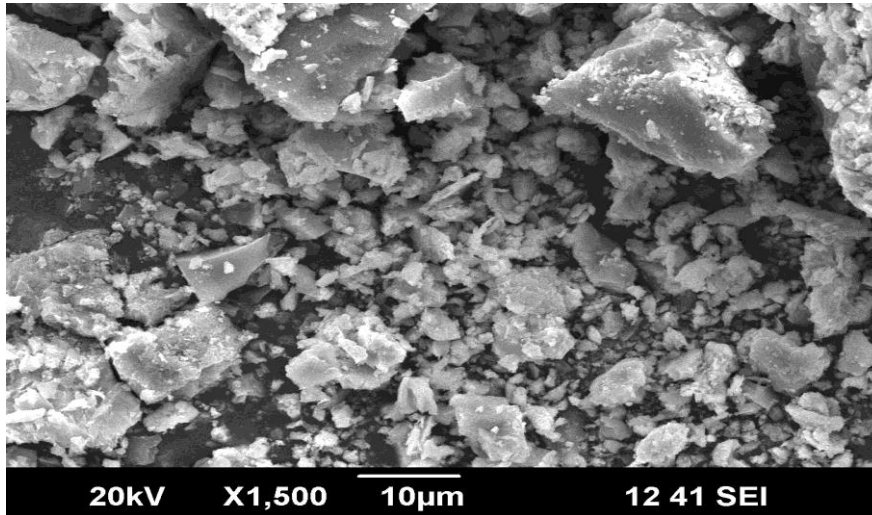


Figure 1.c SEM micrograph of the ZnWO<sub>4</sub>

The Figure 1.c has shown the SEM micrograph of the ZnWO<sub>4</sub>. The Figure 1.c is represent, the SEM micrograph of ZnWO<sub>4</sub> shown semi crystalline nature [6-12].

### FTIR Analysis

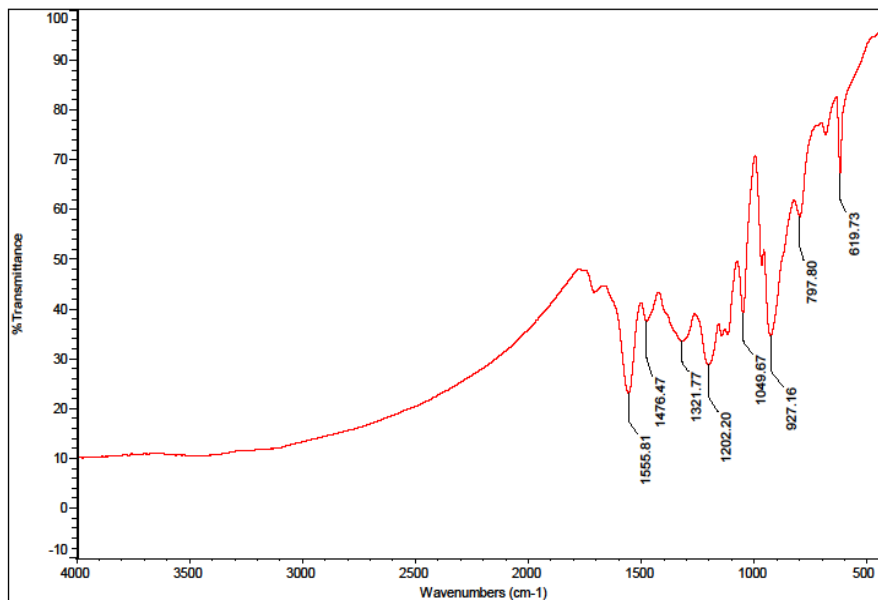


Figure 2.a FTIR spectrum of the pure PPy

The Figure 2.a has shown the FTIR spectra of pure PPy. Characteristic frequencies were observed at 1555 cm<sup>-1</sup>, 1476 cm<sup>-1</sup>, 1321 cm<sup>-1</sup>, 1202 cm<sup>-1</sup>, 1049 cm<sup>-1</sup>, 927 cm<sup>-1</sup>, 797 cm<sup>-1</sup> 619 cm<sup>-1</sup> for pure PPy.

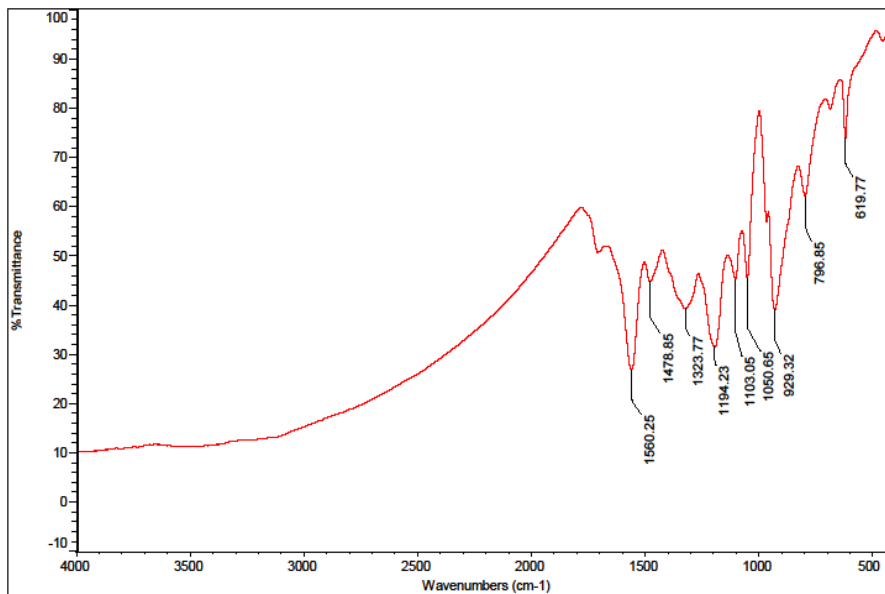


Figure 2.b FTIR spectrum of the PPy/ZnWO<sub>4</sub> (wt. 50%) composite

The Figure 2.b has shown the FTIR spectra of, PPy/ZnWO<sub>4</sub> (wt. 50%) composite. Characteristic frequencies were observed at 1567 cm<sup>-1</sup>, 1480 cm<sup>-1</sup>, 1328 cm<sup>-1</sup>, 1198 cm<sup>-1</sup>, 1109 cm<sup>-1</sup>, 1052 cm<sup>-1</sup>, 931 cm<sup>-1</sup>, 801 cm<sup>-1</sup> & 619 cm<sup>-1</sup> for PPy/ ZnWO<sub>4</sub> (wt. 50%) composite. may be attributed due to the presence of C=N stretching, N-H bending deformation, C-N stretching and C-H bending deformation frequencies. The stretching frequencies were shifted towards higher frequency side when pure PPy was compared with PPy/ZnWO<sub>4</sub> (wt. 50%) composite. This indicates that, there is homogeneous distribution of ZnWO<sub>4</sub> particles in the polymeric chain due to the Van der Waals interaction between polypyrrole chain and ZnWO<sub>4</sub> [6-7, 10-14].

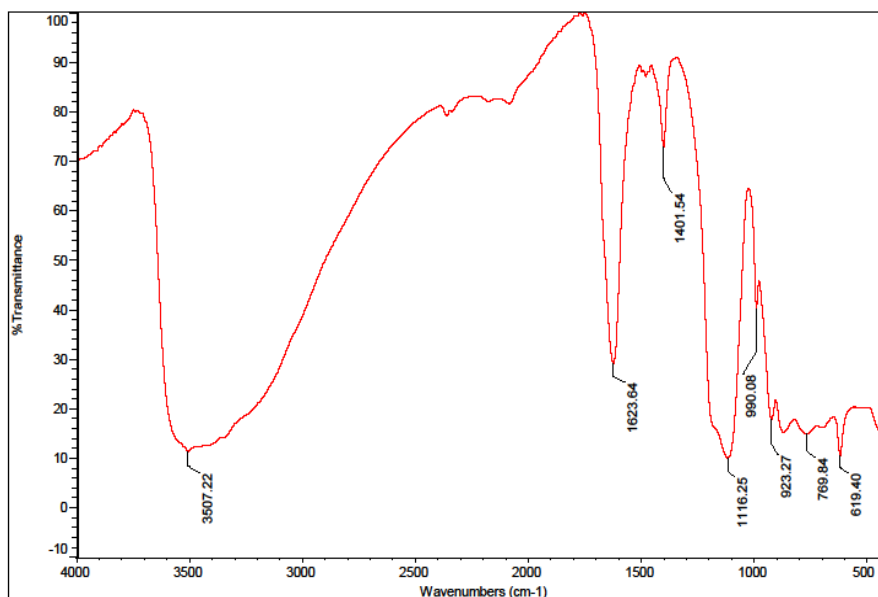


Figure 2.c FTIR spectrum of the ZnWO<sub>4</sub>

**International Journal of Innovative Research in Science,  
Engineering and Technology**

(An ISO 3297: 2007 Certified Organization)

Vol. 3, Issue 6, June 2014

The Figure 2.c has shown the FTIR spectra of ZnWO<sub>4</sub>. Characteristic frequencies were observed at 1518 cm<sup>-1</sup>, 1360 cm<sup>-1</sup>, 1049 cm<sup>-1</sup>, 963 cm<sup>-1</sup>, 911 cm<sup>-1</sup>, 842 cm<sup>-1</sup> & 615 cm<sup>-1</sup> for ZnWO<sub>4</sub>. This shown that, there is homogeneous distribution of ZnWO<sub>4</sub> particles in the polymeric chain. So, particles of ZnWO<sub>4</sub> in pure PPy have shown that, ZnWO<sub>4</sub> particles have strong influence on pure PPy.

*XRD Analysis*

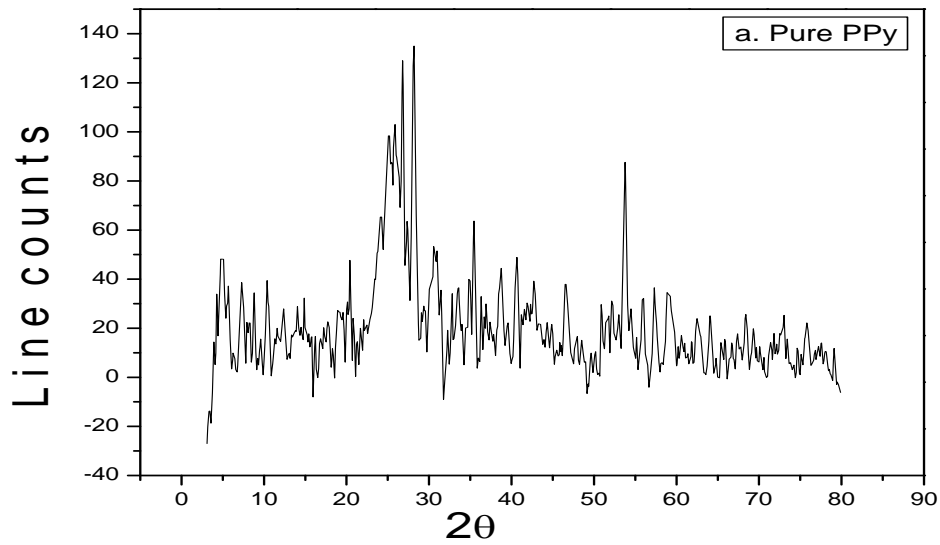


Figure 3.a XRD pattern of the pure PPy

The Figure 3.a represents the XRD pattern of pure PPy. This has a broad peak at about 2θ=25°, shown a characteristic peak of amorphous PPy.

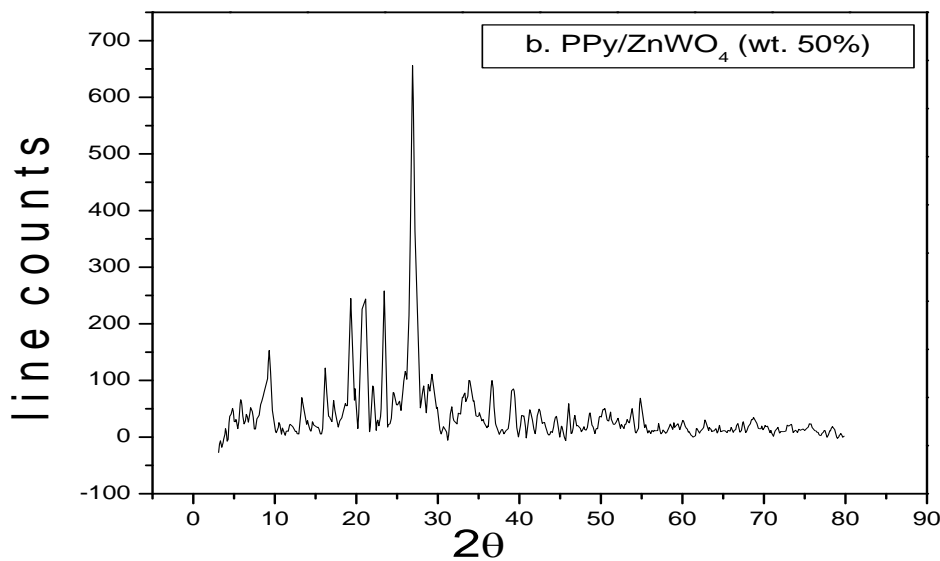


Figure 3.b XRD pattern of the PPy/ ZnWO<sub>4</sub> (wt. 50%) composite

## International Journal of Innovative Research in Science, Engineering and Technology

(An ISO 3297: 2007 Certified Organization)

Vol. 3, Issue 6, June 2014

The XRD pattern of PPy/ZnWO<sub>4</sub> (50 wt. %) composite shown in the Figure 3.b. The characteristic peaks were indexed by lattice parameter values. The main peaks were observed with 2θ at 9.31°, 13.32°, 16.19°, 19.32°, 21.12°, 23.39°, 26.89°, 31.66°, 36.63°, 39.24°, 41.32°, 46.06°, and 54.85° with respect to inter-planar spacing (d) 9.48 Å, 6.64 Å, 5.46 Å, 4.59 Å, 4.20 Å, 3.79 Å, 3.31 Å, 2.82 Å, 2.45 Å, 2.29 Å, 2.18 Å, 1.96 Å, and 1.67 Å respectively. Careful analysis of the XRD of the PPy/ZnWO<sub>4</sub> (50 wt. %) composite suggests that, it exhibits semi-crystalline behaviour.

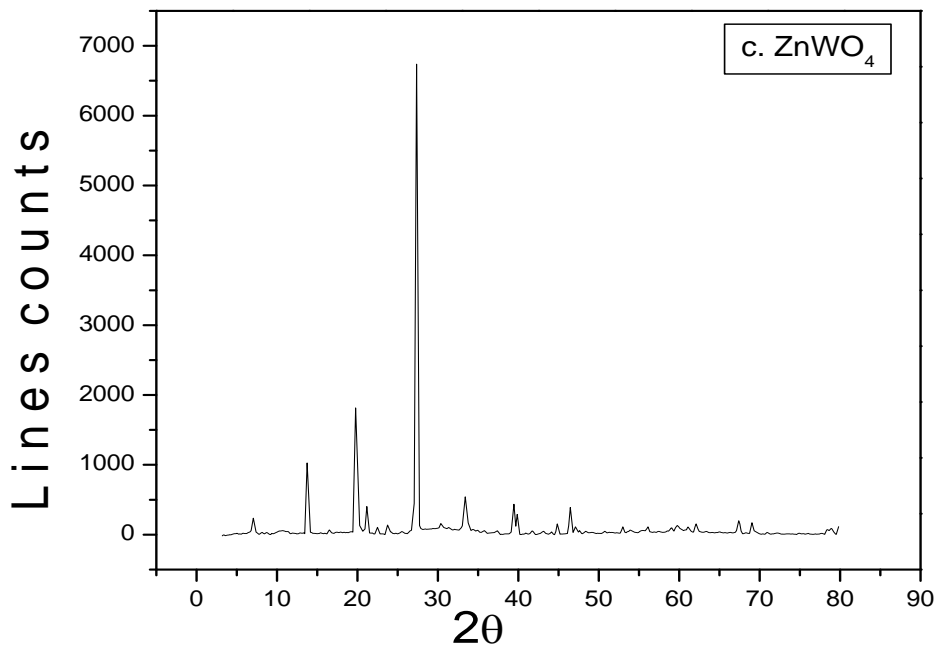


Figure 3.c XRD pattern of the ZnWO<sub>4</sub>

Figure 3.c XRD pattern of the ZnWO<sub>4</sub>. The Figure 3.c represents the XRD pattern of the ZnWO<sub>4</sub> revealing the semi-crystalline nature [6-11].

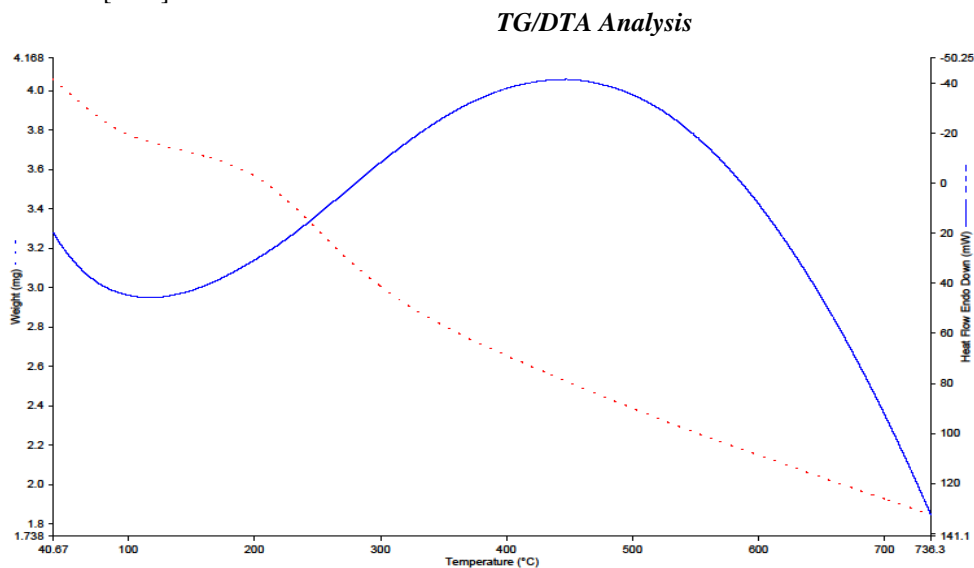


Figure 4.a TG/DTA thermograph of the pure PPy

# International Journal of Innovative Research in Science, Engineering and Technology

(An ISO 3297: 2007 Certified Organization)

Vol. 3, Issue 6, June 2014

The most important and reliable factor in the study of heat stable polymers is the measurement or evaluation of thermal stability. Thermal properties and interaction between the polymers can also be noted from the oxidative degradation curves through thermo-gravimetric analysis (TG/DTA) studies. DTA is most commonly used to determine transition temperatures such as glass transitions, melting cross-linking reactions and decomposition. However, it measures only the total heat flow and the sum of all thermal transitions in the sample. The representative TG/DTA curve for pure PPy is shown in Figures 4.a. The materials have been heated from 40 °C to 740 °C under a constant heating rate of 10 °C/min and in the inert atmosphere of nitrogen gas. Variation of weight is almost linear and the maximum polymer decomposition temperature is there from 40 °C to 740 °C for all. In the Figure 4.a, two major weight loss stages for PPy were observed at 110 °C to 130°C and 736.3°C.

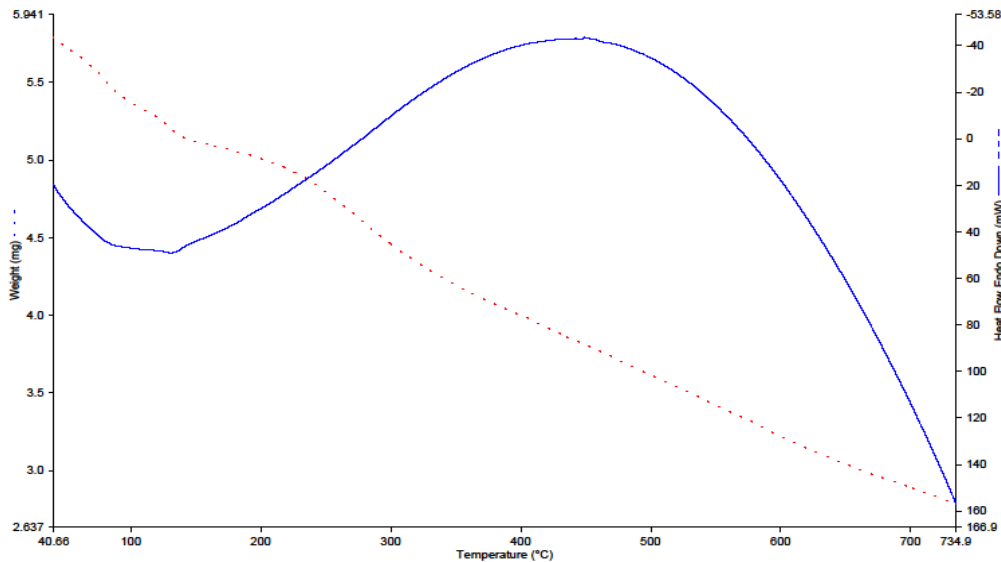


Figure 4.b TG/DTA thermograph of the PPy/ZnWO<sub>4</sub> (wt. 50%) composite

The Figure 4.b is shown the TG/DTA thermograph of the PPy/ZnWO<sub>4</sub> (wt. 50%) composite. In the Figure 4.b, two major weight loss stages for PPy/ZnWO<sub>4</sub> were observed at 135°C to 145°C and 734.8°C.

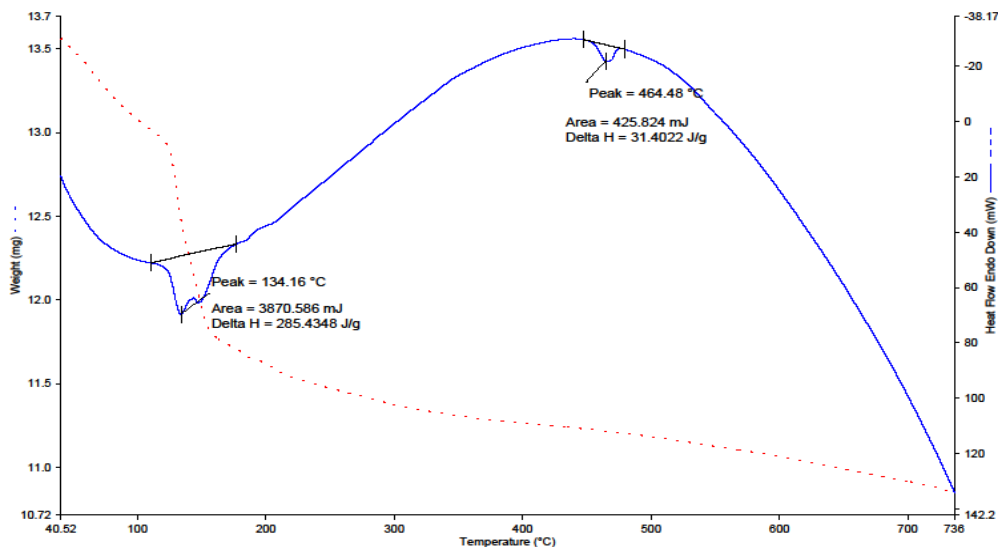


Figure 4.c TG/DTA thermograph of the ZnWO<sub>4</sub>



# International Journal of Innovative Research in Science, Engineering and Technology

(An ISO 3297: 2007 Certified Organization)

Vol. 3, Issue 6, June 2014

The Figure 4.c is shown the TG/DTA thermograph of the ZnWO<sub>4</sub>. And in the Figure 4.c, three major weight loss stages for PPy/ZnWO<sub>4</sub> were observed at 130°C to 134.16°C, 464.48 °C and 734.5 °C.

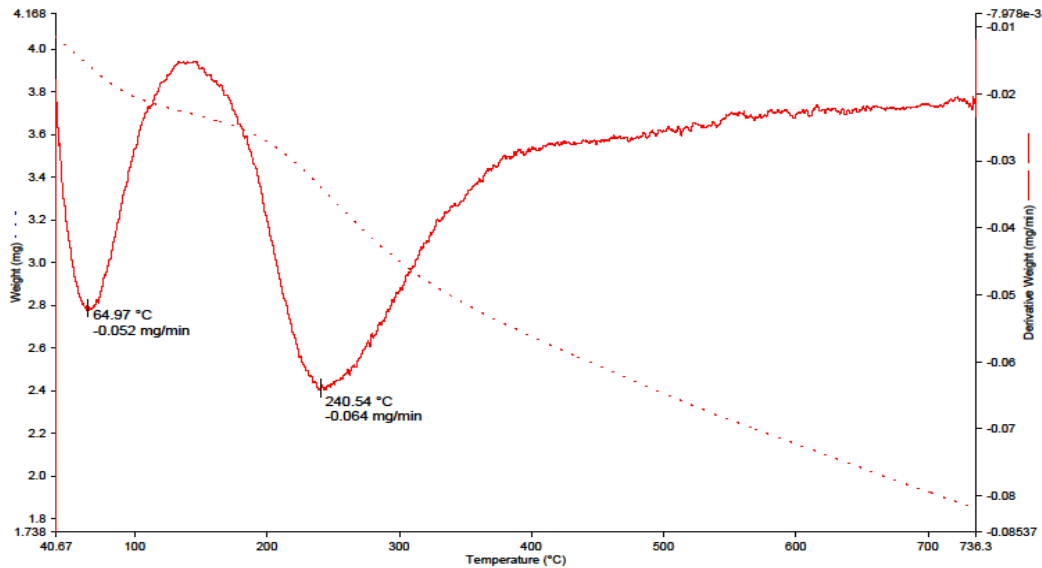


Figure 5.a TG/DTA thermograph of the pure PPy

Derivative weight (mg/min) versus temperature is shown in Figures 5.a for the pure PPy. For pure PPy, 0.052 mg/min is decomposed at 64.97 °C mg/min and 0.064 mg/min is decomposed at 240.54 °C with respect to total weight of the sample i.e. 4.057 mg.

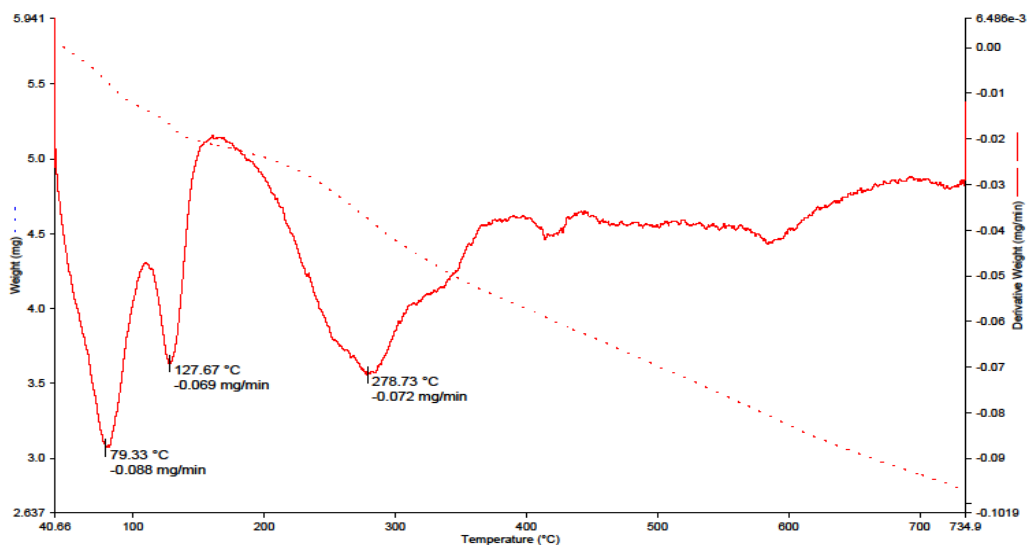


Figure 5.b TG/DTA thermograph of the PPy/ZnWO<sub>4</sub> (wt. 50%) composite

Derivative weight (mg/min) versus temperature is shown in Figures 5.b for the PPy/ZnWO<sub>4</sub> (wt. 50%) composite. For PPy/ZnWO<sub>4</sub> (wt. 50%) composite, 0.088 mg/min is decomposed at 79.33 °C mg/min, 0.069 mg/min is

# International Journal of Innovative Research in Science, Engineering and Technology

(An ISO 3297: 2007 Certified Organization)

Vol. 3, Issue 6, June 2014

decomposed at 127.67 °C mg/min and 0.072 mg/min is decomposed at 278.73 °C with respect to total weight of the sample i.e. 5.791 mg.

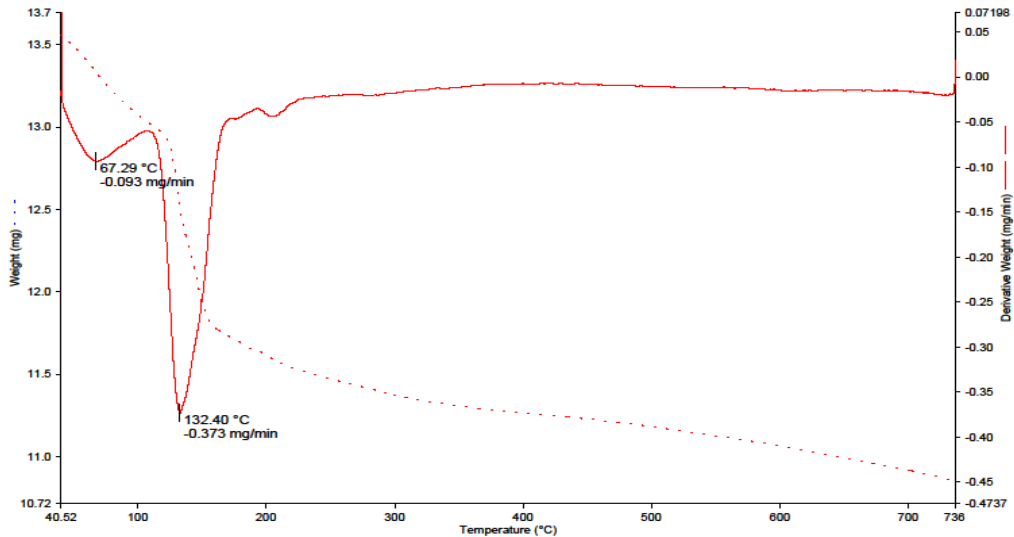


Figure 5.c TG/DTA thermograph of the ZnWO<sub>4</sub>

Derivative weight (mg/min) versus temperature is shown in Figures 5.c for ZnWO<sub>4</sub>. For ZnWO<sub>4</sub>, 0.093 mg/min is decomposed at 67.29 °C mg/min and 0.373 mg/min is decomposed at 132.40 °C with respect to total weight of the sample i.e. 13.56 mg.

It is found that, the weight loss caused by the volatilization of the small molecules in PPy/ZnWO<sub>4</sub> (wt. 50%) composite at different temperatures is slow compared to that of pure PPy and indicates its higher stability, which clearly proves that ZnWO<sub>4</sub> was inserted into the PPy to form composite and has increased the thermal stability of the composite material [15-23].

### Dielectric Property Study

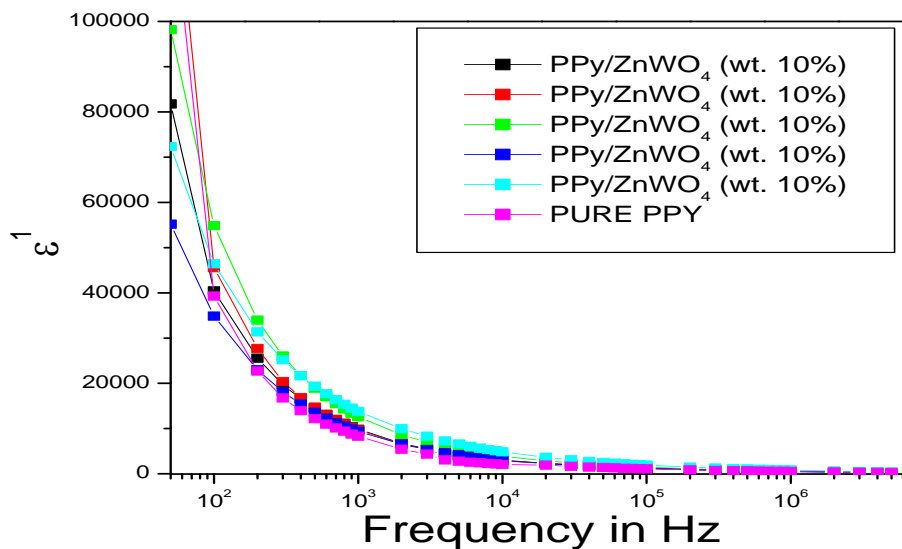


Figure 6.a Variation of  $\epsilon^1$  as a function of frequency for the PPy and PPy/ZnWO<sub>4</sub> composites

## International Journal of Innovative Research in Science, Engineering and Technology

(An ISO 3297: 2007 Certified Organization)

Vol. 3, Issue 6, June 2014

The Figure 6.a has shown the variation of  $\epsilon^1$  is a function of frequency for the PPy and PPy/ZnWO<sub>4</sub> composites. The variation of the dielectric relative permittivity ( $\epsilon^1$ ) as a function of frequency for the pure PPy and PPy/ZnWO<sub>4</sub> composites decreases with the increasing of frequency.

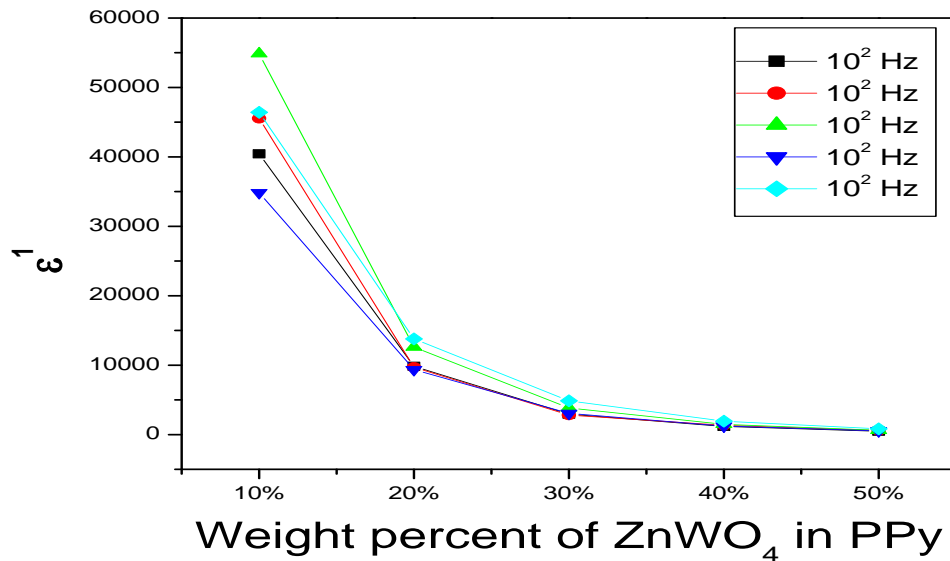


Figure 6.b Variation of  $\epsilon^1$  as a function of wt. % of PPy/ ZnWO<sub>4</sub> composites

The variation of  $\epsilon^1$  is a function of wt. % of PPy/ZnWO<sub>4</sub> composites is shown in the Figures 6.b. The variation of the dielectric relative permittivity ( $\epsilon^1$ ) is a function of wt. % of PPy/ZnWO<sub>4</sub> composites decreases with the increasing of frequency.

This may be attributed to the tendency of dipoles in polymeric samples to orient themselves in the direction of the applied field. However, the decreasing trend seems not too sharp as compared for lower frequency region at the high frequency range (10<sup>4</sup> Hz to 10<sup>6</sup> Hz). This trend is observed for all graphs for different concentration of dopants. It could be explained by dipoles orientation, which difficult to rotate at high frequency range. On the other hand, the high value of  $\epsilon^1$  at low frequency might be due to the electrode effect and interfacial effect of the sample [24-26].

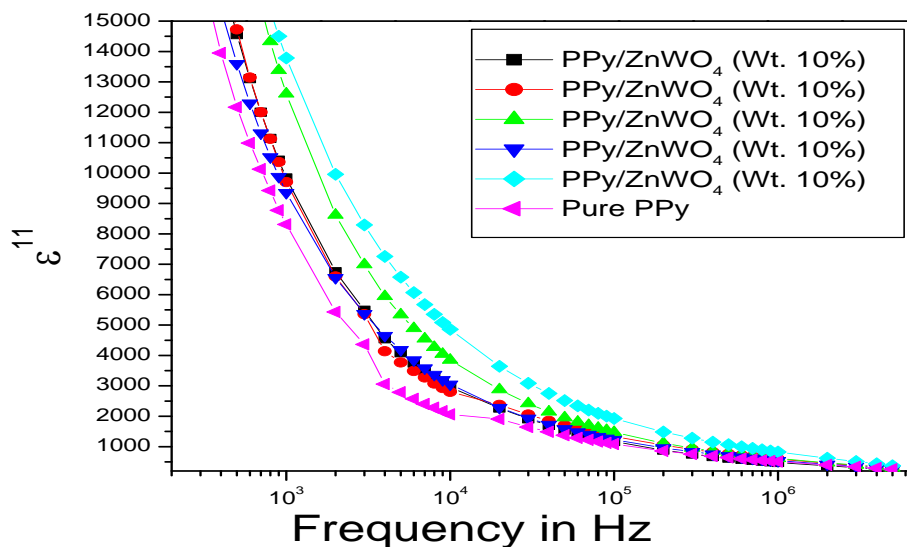


Figure 7.a Variation of  $\epsilon^{11}$  is a function of frequency for PPy and PPy/ZnWO<sub>4</sub> composites

## International Journal of Innovative Research in Science, Engineering and Technology

(An ISO 3297: 2007 Certified Organization)

Vol. 3, Issue 6, June 2014

The variation of dielectric loss ( $\epsilon''$ ) is a function of frequency for the PPy and PPy/ZnWO<sub>4</sub> composites shown in the Figure 7.a. It is clear from the graph that, the dielectric loss decreases with frequency. The larger value of loss factor or dielectric loss at low frequency could be due to the mobile charges within the polymer backbone. The higher value of the dielectric loss for the higher concentration of dopant can be understood in terms of electrical conductivity, which is associated with the dielectric loss.

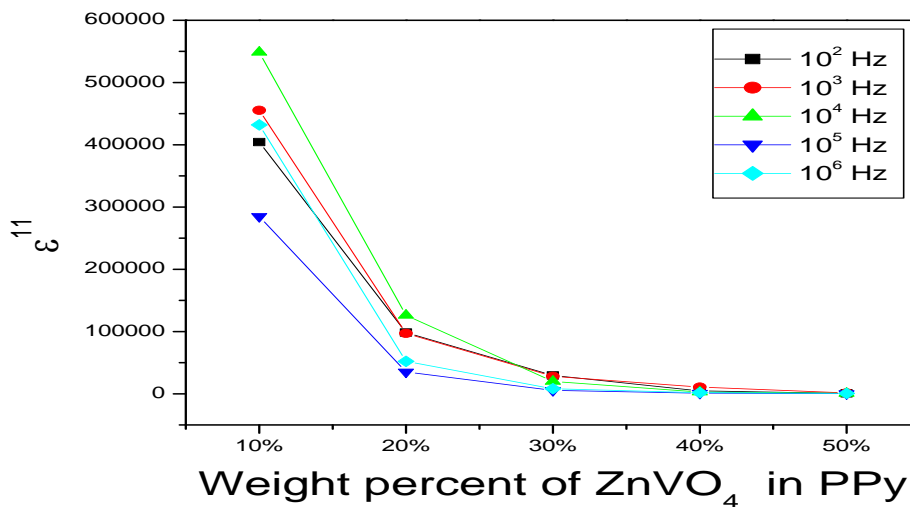


Figure 7.b Variation of  $\epsilon''$  as a function of wt. % of PPy/ZnWO<sub>4</sub> composites

The variation of dielectric loss ( $\epsilon''$ ) is a function of wt. % of PPy/ZnWO<sub>4</sub> composites for the PPy and PPy/ZnWO<sub>4</sub> composites decreases with the increasing of frequency were shown in the Figure 7.b. On the other hand, the mobile charges i.e. polarons that belong to conducting PPy and free ions that come from ammonium persulphate increase at higher concentration of the dopant thus also influence lower value of  $\epsilon''$  at high frequency. Moreover, the ZnWO<sub>4</sub> exhibits flexible polar side groups with polar bond as the bond rotating having intense dielectric  $\alpha$ -transition. Thus, there is a change in the chemical composition of the polymer repeated unit due to the formation of hydrogen bonds with hydroxyl groups in the polymerization process, which in turn makes the polymer chain flexible and hence, enhances the electrical conductivity [25-27].

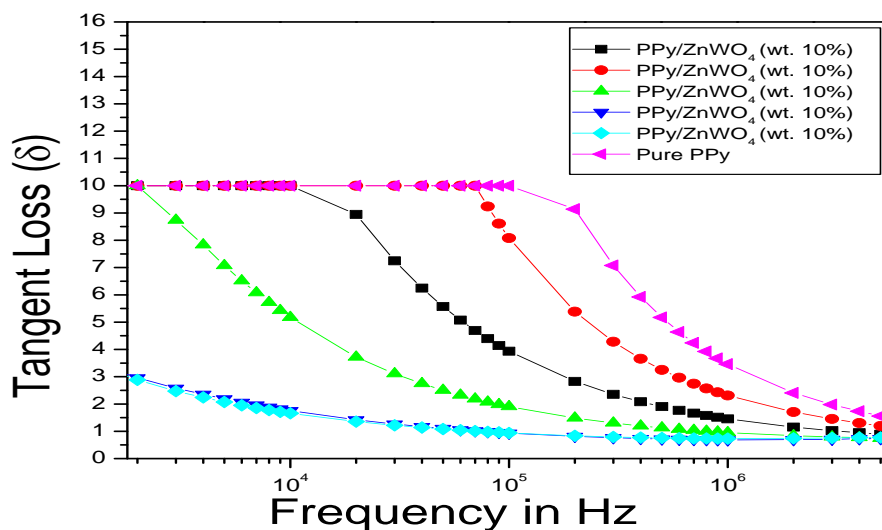


Figure 8 Variation of tangent loss as a function of frequency for the PPy and PPy/ZnWO<sub>4</sub> composites

# International Journal of Innovative Research in Science, Engineering and Technology

(An ISO 3297: 2007 Certified Organization)

Vol. 3, Issue 6, June 2014

The Figure 8 is shown the variation of tangent loss as a function of frequency for the PPy and PPy/ZnWO<sub>4</sub> composites. One can conclude that with the increasing amount of the dopant, the tangent loss ( $\delta$ ) is relatively reduced although it does not change for the whole samples as it is might be due to intrinsic behaviour of the sample. These results confirm the explanation for the dielectric relative permittivity ( $\epsilon^1$ ) and dielectric loss ( $\epsilon^{11}$ ) characteristics as tangent loss ( $\delta$ ) decreases with the increasing composition of the dopant [20, 24-28].

## IV. CONCLUSION

The PPy/ZnWO<sub>4</sub> composites were synthesized to tailor the transport properties. Detailed characterizations of the composites were carried out using SEM, FTIR, XRD and TG/DTA techniques. The results of dielectric relative permittivity ( $\epsilon^1$ ) and dielectric loss ( $\epsilon^{11}$ ) of PPy/ZnWO<sub>4</sub> composites show a strong dependence on the weight percent of ZnWO<sub>4</sub> in polypyrrole. PPy/ZnWO<sub>4</sub> composites may find applications in sensors.

## ACKNOWLEDGEMENT

The authors would like to acknowledge The Principal, BMSCE, BMSET, Bangalore-560019 for their cooperation and help. FTIR, TGA, SEM and XRD analysis of the samples were carried out at Sophisticated Analytical Instruments Facility (SAIF) of Cochin University of Science And Technology, Cochin, India. The author<sup>1</sup> thank to wife and children for cooperation.

## REFERENCES

- [1]. A TerjeSkotheim and R John Reynolds, *Handbook of Conducting Polymers Third Edition Conjugated Polymers*, (CRC Press Inc., USA, 2006)
- [2]. MohdHamzahHarun, Elias Saion, AnuarKassim, NoorhanaYahya and Ekramul Mahmud, *JASA-2*, 63, (2007)
- [3]. GyörgyInzelt, *J. Solid State Electrochem*, 15, 1711 (2011)
- [4]. R Struëmpeler and J Glatz-reichenbach, *J. of Electro-ceramics*, 3(4), 329 (1999)
- [5]. A K Bhakshi, *Bull. Mater. Sci.*, 18(5), 469 (1995)
- [6]. Reza Ansari, *E-Journal of Chemistry*, 3, 186 (2006)
- [7]. V K Gade, D J Shirale, P D Gaikwad, K P Kakde, P A Savale, H J Kharat, B H Pawar and M D Shirsat, *Int. J. Electrochem. Sci.*, 270 (2007)
- [8]. M V Murugendrappa and M V N Ambika Prasad, *J. App. Poly. Sci.*, 103, 2797 (2007)
- [9]. T K Vishnuvardhan, V R Kulkarni, C Basavaraja and S C Raghavendra, *Bull. Mater. Sci.*, 29(1), 77 (2006)
- [10]. M V Murugendrappa, Syed Khasim and M V N Ambika Prasad, *Bull. Mater. Sci.*, 28(6), 565 (2005)
- [11]. Himanshu Narayan, Angela M Montano, Monica L Hernandez, July A Hernandez, Claudia P Gonzalez and Cesar A Ortiz, *J. Mater. Environ. Sci.*, 3(1), 137 (2012)
- [12]. Qunwei Tang, Xiaoming Sun, Qinghua Li, Jianming Lin and Jihuai Wu, *J. Mater. Sci.*, 44, 849 (2009)
- [13]. Qingzhi Luo, Xueyan Li, Desong Wang, Yanhong Wang and Jing An, *J. Mater. Sci.*, 46, 1646 (2011)
- [14]. Lunhong Ai and J Jiang, *J. Mater. Sci.: Mater. Electron*, 21, 410 (2010)
- [15]. S HosseinHosseini and A Ali Entezami, *Iranian Polymer Journal*, 14(3), 201 (2005)
- [16]. Nakamura O, Ogino I and Kodama T, *Solid State Ionics*, 3-4, 347 (1981)
- [17]. Doyle CD, *Anal Chem*, 3, 77 (1961)
- [18]. Juan C Apesteguy and Silvia E Jacobo, *J. Mater. Sci.*, 42, 7062 (2007)
- [19]. Mohammad Sideeq Rather, Kowsar Majid, Ravinder Kumar Wanchoo and Madan LalSingla, *J. Therm. Anal Calorim.*, 112, 893 (2013)
- [20]. S Anoop Kumar, AvanishPratap Singh, Parveen Saini, FehmeedaKhatoun and S Dhawan, *J. Mater. Sci.*, 47, 2461 (2012)
- [21]. Nikola Perinka, MarketaDrzkova, Milena Hajna and BohumilJasurek, *J. Therm. Anal Calorim.*, 116, 589 (2014)
- [22]. Zihang Huang, Shaoxu Wang, Hui Li, Shihui Zhang and Zhicheng Tan, *J. Therm. Anal Calorim.*, 115, 259 (2014)
- [23]. SamranaKazim, Shahzada Ahmad, Jiri Pflieger, Josef Plestil and Yogesh M Joshi, *J. Mater. Sci.*, 47, 420 (2012)
- [24]. Dutta P, Biswas S and De S K, *Materials Research Bulletin*, 37 (2002)
- [25]. MohdHamzahHarun, Elias Saion, AnuarKassim, Ekramul Mahmud, MuhdYousuf Hussain, and IskandarShahrim Mustafa, *J. For The Advancement OF Science & Arts*, 1(1), 9 (2009)
- [26]. Havriliak S and S Negami, *Polymer*, 8, 161 (1967)
- [27]. Singh K P and Gupta P N, *European Polymer Journal*, 34, 1023 (1998)
- [28]. M L Singla, Rajeev Sehrawat, NidhiRana and Kulvir Singh, *J. Nanopart Res.*, 13, 2109 (2011)